

Platinum covalent shell cross-linked micelles designed to deliver doxorubicin for synergistic combination cancer therapy

Caiying Zhu^{1,*}Jingjing Xiao^{1,*}Ming Tang²Hua Feng¹Wulian Chen³Ming Du¹

¹Medical Center of Diagnosis and Treatment for Cervical Diseases, Obstetrics and Gynecology Hospital, Shanghai Medical College, Fudan University, Shanghai, ²Department of Otorhinolaryngology-Head and Neck Surgery, Ningbo Medical Center, Li Huli Hospital, Ningbo, ³State Key Laboratory of Molecular Engineering of Polymers, Department of Macromolecular Science, Fudan University, Shanghai, China

*These authors contributed equally to this work

Abstract: The preparation of polymer therapeutics capable of controlled release of multiple chemotherapeutic drugs has remained a tough problem in synergistic combination cancer therapy. Herein, a novel dual-drug co-delivery system carrying doxorubicin (DOX) and platinum(IV) (Pt[IV]) was developed. An amphiphilic diblock copolymer, PCL-b-P(OEGMA-co-AzPMA), was synthesized and used as a nanoscale drug carrier in which DOX and Pt(IV) could be packaged together. The copolymers were shell cross-linked by Pt(IV) prodrug via a click reaction. Studies on the in vitro drug release and cellular uptake of the dual-drug co-delivery system showed that the micelles were effectively taken up by the cells and simultaneously released drugs in the cells. Furthermore, the co-delivery polymer nanoparticles caused much higher cell death in HeLa and A357 tumor cells than either the free drugs or single-drug-loaded micelles at the same dosage, exhibiting a synergistic combination of DOX and Pt(IV). The results obtained with the shell cross-linked micelles based on an anticancer drug used as a cross-linking linkage suggested a promising application of the micelles for multidrug delivery in combination cancer therapy.

Keywords: dual-drug co-delivery system, amphiphilic diblock copolymer, shell cross-linked micelles, synergistic combination cancer therapy

Abbreviations

ATRP, atom transfer radical polymerization; AzPMA, 3-azidopropyl methacrylate; CL, caprolactone; DAPI, 4',6-diamidino-2-phenylindole; DDSs, controlled drug delivery systems; DLS, dynamic light scattering; DMF, dimethylformamide; DOX, doxorubicin; DP, degree of polymerization; EE, encapsulation efficiency; FT-IR, Fourier transform infrared; GPC, gel permeation chromatography; ¹H NMR, proton nuclear magnetic resonance; HBMP, 2-hydroxyethyl 2-bromo-2-methylpropanoate; LE, loading efficiency; MDR, multidrug resistance; M_n , average number molecular weight; MWCO, molecular weight cut-off; NCL, non-cross-linked; NHS, N-hydroxysuccinimide; OEGMA, oligo(ethylene glycol) ethyl methacrylate; PAzPMA, poly(AzPMA); PBS, phosphate-buffered saline; PCL, polycaprolactone; PDI, polydispersity index; PEG, poly(ethylene glycol); PMDETA, *N,N,N',N'',N'''*-pentamethyldiethylenetriamine; POEGMA, poly(OEGMA); Pt(IV), platinum(IV); PTX, paclitaxel; ROP, ring-opening polymerization; SCL, shell cross-linked; TEM, transmission electron microscopy; TGA, thermogravimetric analysis; THF, tetrahydrofuran; ZnPc, zinc-phthalocyanine.

Introduction

The use of most chemotherapeutic drugs is limited by severe side effects, low therapeutic index and development of drug resistance.¹⁻³ Driven by an urgent need for practical

Correspondence: Ming Du
Obstetrics and Gynecology Hospital,
Shanghai Medical College, Fudan
University, Da Lin Road, No 358,
Shanghai 200011, China
Tel/fax +86 21 6345 0944
Email duming0111@126.com

applications in chemotherapy, effective DDSs have been developed. Over the past few decades, DDSs have successfully improved the therapeutic efficiency of chemotherapeutic drugs by improving drug solubility, reducing systemic toxicity, increasing circulation time in the blood and controlling drug release profile.⁴⁻⁷ However, due to the ability of the tumor cells to develop MDR, traditional DDSs used for the delivery of single chemotherapeutic drug cannot prevent MDR, which ultimately leads to treatment failure in most cancer therapy.⁸⁻¹⁰

In principle, chemotherapeutic drugs with different activities delivered simultaneously to the same cancer cells can maximize cytotoxicity and reduce dosage of each drug.^{11,12} Furthermore, synergistic combination therapy can also minimize the chance of developing resistance to any one drug by the cells. Thus, the use of nanoparticle-based multidrug co-delivery systems has been proposed to overcome undesirable toxicity and MDR in the modern clinical cancer therapy.¹³⁻¹⁵ To date, among the amounts of drug carriers, polymeric micelles have been widely employed in the development of multidrug co-delivery systems due to many advantages, such as core-shell nanostructures, excellent biocompatibility, biodegradability and versatile chemistry for further functionalization.^{16,17} In addition, they are of nanoscopic size and stealthy property. Thus, polymeric micelles usually lead to a prolonged blood circulation and passive accumulation in solid tumor through the enhanced permeability and retention effect.¹⁸⁻²⁰ These features make polymeric micelles the preferred choice for drug delivery purposes. For example, Wang et al have reported that an amphiphilic copolymer PEG-poly(lactide-co-glycolide) could co-deliver hydrophilic DOX and hydrophobic PTX by improved double-emulsion method, showing a synergistic effect and enhanced antitumor efficacy.²¹ Conte et al developed a dual carrier system for co-delivery of DOX and photosensitizer ZnPc based on a biodegradable amphiphilic block copolymer, PEG-b-PCL.²² The ZnPc/DOX-loaded nanoparticles suppressed the growth of tumor cells more efficiently than nanoparticles loaded only with DOX, thus indicating a combined effect of DOX and ZnPc. Although these non-covalent drug-loaded polymeric micelles are easy to fabricate, micelle structural integrity and drug encapsulation stability are of concern. Upon intravenous administration, polymeric micelles will be subjected to a high dilution, ionic strength, and large shear forces. When structural stability of the micelles is affected, the drug burst release is inevitable during blood circulation, leading to undesirable toxicity and a low therapeutic index.²³⁻²⁵

To solve the above-mentioned stability issue of polymeric micelles, shell or core cross-linked micelles have been proposed. After micelles cross-linking, they are found

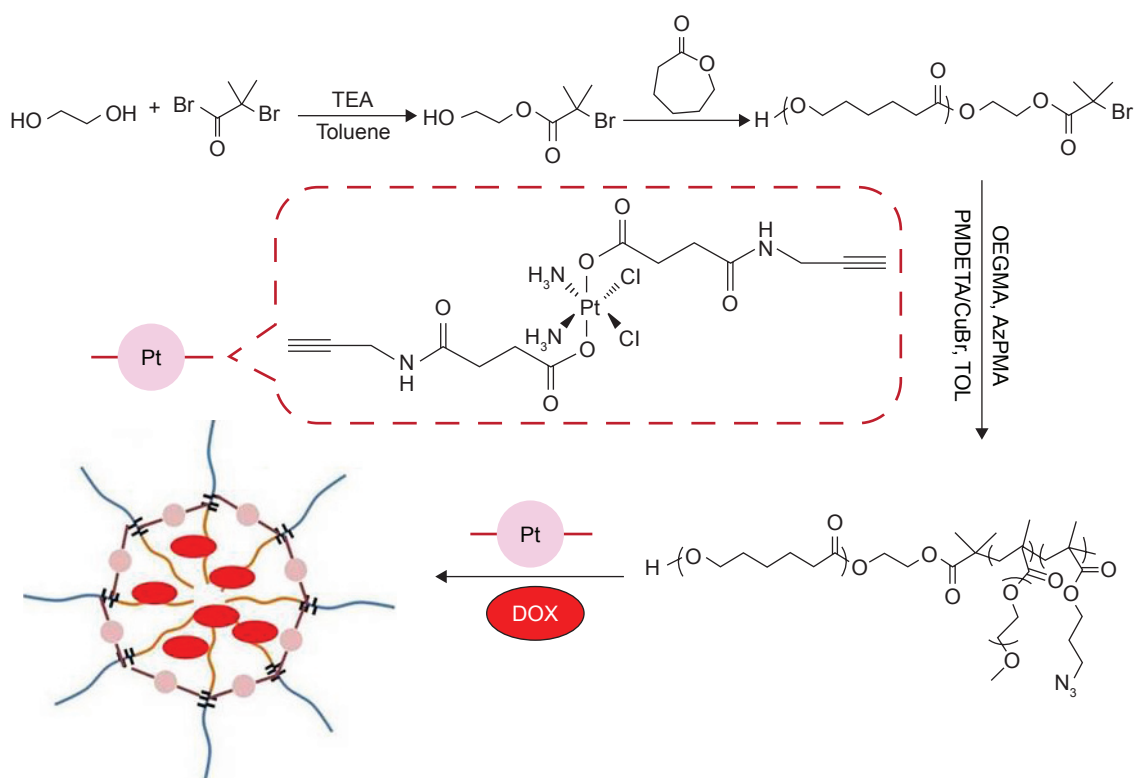
to be stable against disassociation under high dilution, and their aggregation is independent of external influences such as changes in pH values and other interference.²⁶⁻³³ Recently, Liao et al designed core cross-linked polymer micelles carrying DOX, camptothecin and cisplatin for single-nanoparticle combination cancer therapy, but the system was difficult to synthesize.³⁴ As compared to core cross-linked micelles, SCL micelles are facile to load drug via physical entrapment.³⁵⁻³⁸ If chemotherapeutic drugs are employed as the cross-linker in micelles, SCL micelles can easily achieve co-delivery of multiple drugs. Thus, this new co-delivery drug system has two different drug-loading methods, physical entrapment and covalent loading of drug, and thus exhibits different drug release rates. To the best of knowledge, the strategy of using chemotherapeutic drug as a cross-linker in SCL micelles to construct novel multidrug co-delivery systems is rarely reported. Therefore, it is still a promising challenge in combination cancer therapy.

It is worth noting that the drugs chosen for combination therapy should have nonoverlapping toxicity profiles.³⁹⁻⁴¹ The side effects of DOX mainly arise from cardiotoxicity, while those of cisplatin result from neurotoxicity. Thus, the combination of DOX and cisplatin could show a highly synergistic potency, and suppress the growth of tumor cells more efficiently than a single drug.⁴¹⁻⁴³ In this study, chemotherapeutic drug was utilized as a cross-linker to construct a novel dual-drug co-delivery system for the combined delivery of DOX and Pt(IV). The amphiphilic diblock copolymer PCL-b-P(OEGMA-co-AzPMA) was synthesized, and then DOX was encapsulated in the hydrophobic core of the micelles. Incorporation of Pt(IV) prodrug and shell cross-linking were simultaneously carried out via a click reaction of the azide group in the shell of the micelles with alkyne groups in Pt(IV) prodrug (Scheme 1). The unique SCL micelles were well characterized by FT-IR, GPC, TEM and DLS. Studies on the drug release and cellular uptake of the SCL micelles were carefully performed to evaluate the drug release behavior of SCL micelles. Meanwhile, an enhanced therapeutic efficacy was observed in comparison to a single drug, especially at a significantly lower dose.

Materials and methods

Materials

DOX and cisplatin were purchased from Beijing Huafeng United Technology Co., Ltd. OEGMA ($M_n=480$ g/mol, 99%) purchased from Sigma-Aldrich and Co was passed through a neutral alumina column to remove the inhibitor prior to use. Toluene (99%; Aldrich) was refluxed with sodium beads/benzophenone complex and distilled until the solution turned



Scheme 1 Synthesis routes employed for the preparation of dual-drug-loaded shell cross-linked micelles.

Abbreviations: AzPMA, 3-azidopropyl methacrylate; DOX, doxorubicin; OEGMA, oligo(ethylene glycol) ethyl methacrylate; PMDETA, *N,N,N',N',N''*-pentamethyldiethylenetriamine; Pt, platinum; TEA, triethyl alcohol; TOL, toluene.

purple. Copper(I) bromide (99.999%; Aldrich), PMDETA (98%; Aldrich), hydrogen peroxide (30%; J&K CHEMICA), sodium vitamin (VcNa; 99%; Aladdin) and succinic anhydride (99%; Aladdin) were used as received without further purification. AzPMA and the difunctional initiator, HBMP, were synthesized according to literature procedures.^{44,45} A Pt(IV)-containing difunctional alkyne was prepared from cisplatin. The experimental procedure is presented in Supplementary materials.

Preparation of PCL-Br macroinitiator and PCL-b-P(OEGMA-co-AzPMA)

PCL-Br macroinitiator was obtained via the ROP of CL using the difunctional initiator HBMP. In a typical procedure, a dry 50 mL Schlenk flask (flame-dried under vacuum prior to use) was charged with HBMP (0.15 mL, 0.8 mmol), CL (5 mL, 47 mmol) and dry toluene (10 mL). Then, 0.45 mL solution of Sn(Oct)₂ in toluene (30 mg/mL) was added under nitrogen protection. The polymerization lasted for 5 h in an oil bath at 130°C and was terminated by immersing the flask into liquid N₂. The mixture was diluted with THF, and precipitated into an excess of cold diethyl ether. After repeated purification by dissolving in THF and precipitating in cold diethyl ether, a white solid (4.3 g, yield of 81.1%)

was obtained by drying in vacuo overnight. The molecular weight and molecular weight distribution of PCL-Br were determined by GPC using THF as the eluent, revealing an M_n of 7.19 kDa and a PDI of 1.09 (Figure 1).

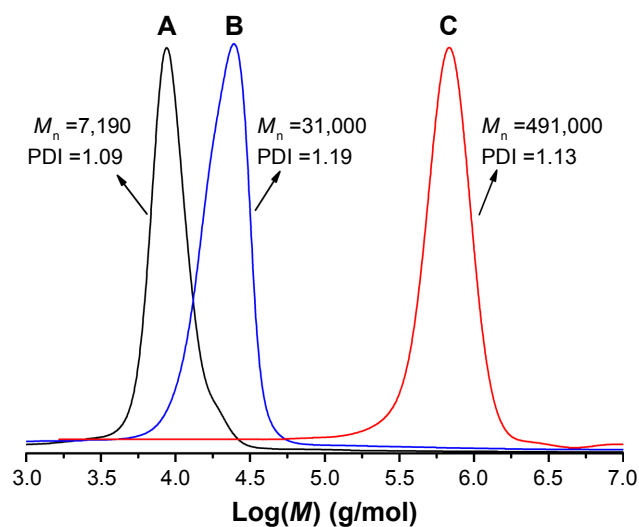


Figure 1 Comparison of gel permeation chromatograms of (A) PCL-Br, (B) PCL-b-P(OEGMA-co-AzPMA) with tetrahydrofuran used as the elute and (C) shell cross-linked micelles with dimethylformamide used as the elute.

Abbreviations: AzPMA, 3-azidopropyl methacrylate; M , molecular weight; M_n , average number molecular weight; OEGMA, oligo(ethylene glycol) ethyl methacrylate; PCL, polycaprolactone; PDI, polydispersity index.

PCL-b-P(OEGMA-co-AzPMA), an amphiphilic diblock copolymer, was prepared by ATRP of AzPMA and OEGMA using PCL-Br as a macroinitiator and CuBr/PMDETA as a catalytic system. Typically, a dry 50 mL Schlenk flask (flame-dried under vacuum prior to use) was charged with PCL-Br (1.25 g, 0.2 mmol) and CuBr (28.6 mg, 0.2 mmol). Then, OEGMA (5.3 mL, 12 mmol), AzPMA (0.5 g, 3 mmol), DMF (15 mL) and PMDETA (0.08 mL, 0.4 mmol) were introduced via a gastight syringe. The mixture was degassed with three freeze–evacuate–thaw cycles followed by immersing into an oil bath at 70°C. The polymerization lasted 12 h and was terminated by immersing the flask into liquid N₂. The mixture was diluted with THF and passed through a short neutral alumina column to remove the residual copper catalyst. The solution was concentrated under vacuum and precipitated into cold diethyl ether. The above dissolution–precipitation cycle was repeated three times. The final product was dried in vacuo overnight, yielding a white viscous solid (4.2 g, yield of 67.2%). The molecular weight and molecular weight distribution were determined by GPC. The GPC was performed at 35°C using THF with an elution rate of 1.0 mL/min on Agilent 1100 equipped with a G1310A pump, a G1362A refractive index detector and a G1314A variable wavelength detector. Polystyrene standard samples were employed for the GPC calibration ($M_n=31,000$ g/mol, PDI = 1.19). ¹H NMR spectra were recorded on a Bruker Avance 400 spectrometer using CDCl₃ as solvent, and trimethylsilane was used as internal standard. ¹H NMR (CDCl₃): 0.77–0.95 (3H, CH₃CCH₂ of POEGMA and PAzPMA), 1.38 (2H, OCH₂CH₂CH₂CH₂CH₂CO of PCL), 1.64 (4H, OCH₂CH₂CH₂CH₂CH₂CO of PCL), 1.95–1.80 (2H, CH₂CCH₃ of POEGMA and PAzPMA), 2.09 (2H, CH₂CH₂N₃), 2.30 (2H, OCH₂CH₂CH₂CH₂CH₂CO of PCL), 3.37 (5H, CH₃O of POEGMA and CH₂CH₂N₃ of PAzPMA), 3.64 (4H, OCH₂CH₂ of POEGMA), 4.06 (2H, OCH₂CH₂CH₂CH₂CH₂CO of PCL). FT-IR spectra were obtained by a NEXUX-470 spectrometer. FT-IR: 2,100 cm⁻¹ (ν_{N₃}).

Preparation of SCL micelles loaded with DOX and Pt(IV)

PCL-b-P(OEGMA-co-AzPMA) (80 mg) and DOX (20 mg) were dissolved in dimethylsulfoxide/DMF (V:V = 1:1), and then deionized water was added dropwise under vigorous stirring. After another 4 h under stirring, the Pt(IV) complex (20 mg, 0.03 mmol), CuSO₄ (5.3 mg, 0.03 mmol) and VcNa (5.94 mg, 0.03 mmol) were added. The reaction mixture was stirred for 24 h at room temperature under N₂ atmosphere. Subsequently, the solution was dialyzed against

deionized water for 3 days (MWCO = 3,500 g/mol), and the deionized water was exchanged every 6 h. Finally, the SCL micelles loaded with DOX and Pt(IV) were obtained by freeze-drying. The size distribution of the micelles was measured by DLS using a Malvern autosizer 4700 instrument. TEM images were obtained on a JEOL 1230 transmission electron microscope, and samples for TEM measurements were prepared by casting a drop of the sample solution on carbon-coated copper grids. The LE of Pt(IV) was determined by TGA. TGA was performed on a Perkin-Elmer Pyris 1 TGA apparatus at a heating rate of 20°C/min from 100 to 800°C under a flow of air. To determine the LE of DOX, the SCL micelle (5 mg) was dispersed in 10 mL of 1 M HCl with 10 mM VcNa and stirred for 3 days at 37°C. Then, the solution was diluted to the concentration of 50 µg/mL, and UV–vis spectroscopy was performed to determine the DOX concentration (maximum absorption at 480 nm), wherein a calibration curve was plotted for DOX/1 M HCl containing 10 mM VcNa solutions with different DOX concentrations. UV–vis absorbance spectra were measured with a Perkin-Elmer Lambda 35 spectrophotometer. The LE (%) was calculated by the following equation:

$$\text{LE (\%)} = \frac{\text{Amount of drug present in nanoparticles}}{\text{Amount of nanoparticles}} \times 100\%$$

The EE was calculated by the following equation:

$$\text{EE (\%)} = \frac{\text{Amount of drug present in nanoparticles}}{\text{Initial amount of drug used to prepare nanoparticles}} \times 100\%$$

According to the above formula, the LE and EE of DOX were 8.5% and 41.0%, respectively, while the LE and EE of Pt(IV) were 8.5% and 35.6%, respectively.

In vitro drug release from SCL micelles

The release of DOX and Pt(IV) from SCL micelles was studied at 37°C in four different medias: (a) PBS of pH 7.4, (b) PBS of pH 7.4 with 5 mM VcNa, (c) PBS of pH 5.5 and (d) PBS of pH 5.5 with 5 mM VcNa. Typically, 20 mg of SCL micelles was dispersed in 4 mL deionized water and was transferred to a dialysis bag with an MWCO of 3,500 g/mol and then immersed in 40 mL of four different media at 37°C with constant shaking. At various time intervals, 10 mL of external medium was withdrawn and replaced with the same volume of fresh buffer solution. Then, an inductively coupled plasma-mass spectrometer was used to determine

the platinum concentration, and UV–vis spectroscopy was performed to determine the DOX concentration.

In vitro cellular uptake and cell assay

The cellular uptake and intracellular release behaviors of SCL micelles loaded with DOX and Pt(IV) were determined using confocal fluorescence microscopy. The HeLa cells were seeded onto glass-bottom petri dishes and incubated at 37°C in an atmosphere containing 5% CO₂ for 24 h to allow cell attachment. The medium was then replaced with 2 mL culture serum-free medium containing SCL micelles sample. After incubation for 6 h, the cells were washed three times with PBS and fixed with paraformaldehyde for 30 min at 4°C, and nuclei were stained with DAPI. Fluorescence images of cells were obtained using confocal fluorescence microscope. The cellular images were acquired with a fluorescence microscope (BX51; Olympus), and the pictures were analyzed using Image-Pro Plus.

HeLa (human cervical carcinoma cells) and A357 (human malignant melanoma cells) were chosen to evaluate the in vitro cytotoxicity of SCL micelles loaded with DOX and Pt(IV) by CCK-8 kit assays. The CCK-8 kit was purchased from Dojindo (Shanghai, China). The cells were seeded in 96-well plates at a density of 1×10⁴ cells/well and incubated at 37°C in an atmosphere containing 5% CO₂ for 24 h to allow cell attachment. Then, the medium was replaced with a fresh medium containing the indicated concentration of SCL micelles. After incubation for 48 and 72 h, the medium was aspirated and replaced by 100 μL of fresh medium containing 10 μL of CCK-8. The cells were incubated for another 2 h at 37°C in dark. Afterward, the absorbance of each well was measured at a wavelength of 450 nm using a microplate reader. The relative cell viability (%) was determined by the following equation:

$$\text{Cell viability (\%)} = \frac{I_{\text{sample}} - I_{\text{blank}}}{I_{\text{control}} - I_{\text{blank}}}$$

where I_{sample} , I_{control} and I_{blank} represent the absorbance intensity, at 450 nm, of cells treated with different samples, control cells (nontreated) and blank well without cells, respectively. The same process was applied to determine the cytotoxicity of PCL-b-P(OEGMA-co-AzPMA) copolymer against HeLa, A357 and HEK-293 (human embryonic kidney) cells. The HeLa, A357 and HEK-293 cell lines were purchased from the Cell Bank of Chinese Academy of Sciences (Shanghai, China).

Results and discussion

Preparation of copolymer and SCL micelles loaded with DOX and Pt(IV)

The synthesis route of PCL-b-P(OEGMA-co-AzPMA) amphiphilic diblock copolymer is illustrated in Scheme 1. Utilizing the bifunctional initiator HBMP, ATRP macro-initiator PCL-Br was synthesized by the ROP of CL. GPC analysis revealed an M_n of 7.19 kDa and a PDI of 1.09. The DP of PCL-Br was determined to be 55, from the ratio of the integration area of the peak at 4.06 ppm (methylene protons adjacent to ester) and that of the peak at 1.95 ppm (methyl protons adjacent to the bromine terminal) in ¹H NMR spectrum (Figure 2A). Thus, the polymer was denoted as PCL₅₅-Br and is abbreviated as PCL-Br in this paper. Then, PCL-b-P(OEGMA-co-AzPMA) amphiphilic diblock copolymer was synthesized via ATRP of OEGMA and AzPMA using PCL-Br as a macroinitiator and CuBr/PMDETA as a catalytic system in DMF at 70°C. As seen from the GPC trace in Figure 1, a monomodal elution peak and a clear shift to the higher molecular weight side were noted, compared with PCL-Br macroinitiator. The chemical structure of PCL-b-P(OEGMA-co-AzPMA) was analyzed by ¹H NMR. As shown in Figure 2B, characteristic signals of PCL, OEGMA and AzPMA were all present. The DP of POEGMA segment was determined to be 40 as indicated by ¹H NMR analysis from the signal integration ratio of peaks at 3.64 ppm (methylene protons of OEGMA units) relative to peak at 4.06 ppm (methylene protons adjacent to ester of PCL block). In the same way, the overall DP of P(OEGMA-co-AzPMA) was calculated to be 53 by ¹H NMR analysis. The polymer was denoted as PCL-b-P(OEGMA_{0.75}-co-AzPMA_{0.25})₅₃ and had an $M_{n,NMR}$ of 27.6 kDa, and is abbreviated as PCL-b-P(OEGMA-co-AzPMA) in this paper. Moreover, a peak at 2,100 cm⁻¹ characteristic of the azide vibration and a peak at 1,110 cm⁻¹ for ether vibration appeared, and the intensity of ester bond at 1,725 cm⁻¹ and alkane at 2,950–2,860 cm⁻¹ also greatly increased after polymerization (Figure 3), indicating the presence of azide group and PEG side chain. These results confirmed that the amphiphilic diblock copolymer PCL-b-P(OEGMA-co-AzPMA) was successfully synthesized.

To prevent drug burst release and achieve co-delivery of DOX and Pt(IV) after intravenous injection, cross-linking of PCL-b-P(OEGMA-co-AzPMA) shell was carried out using Pt(IV) complex containing bifunctional alkyne, which could react with pendent azide groups via azide–alkyne click chemistry to generate Pt(IV) linkages within the hydrophilic shell. The obtained SCL micelles were then characterized by FT-IR,

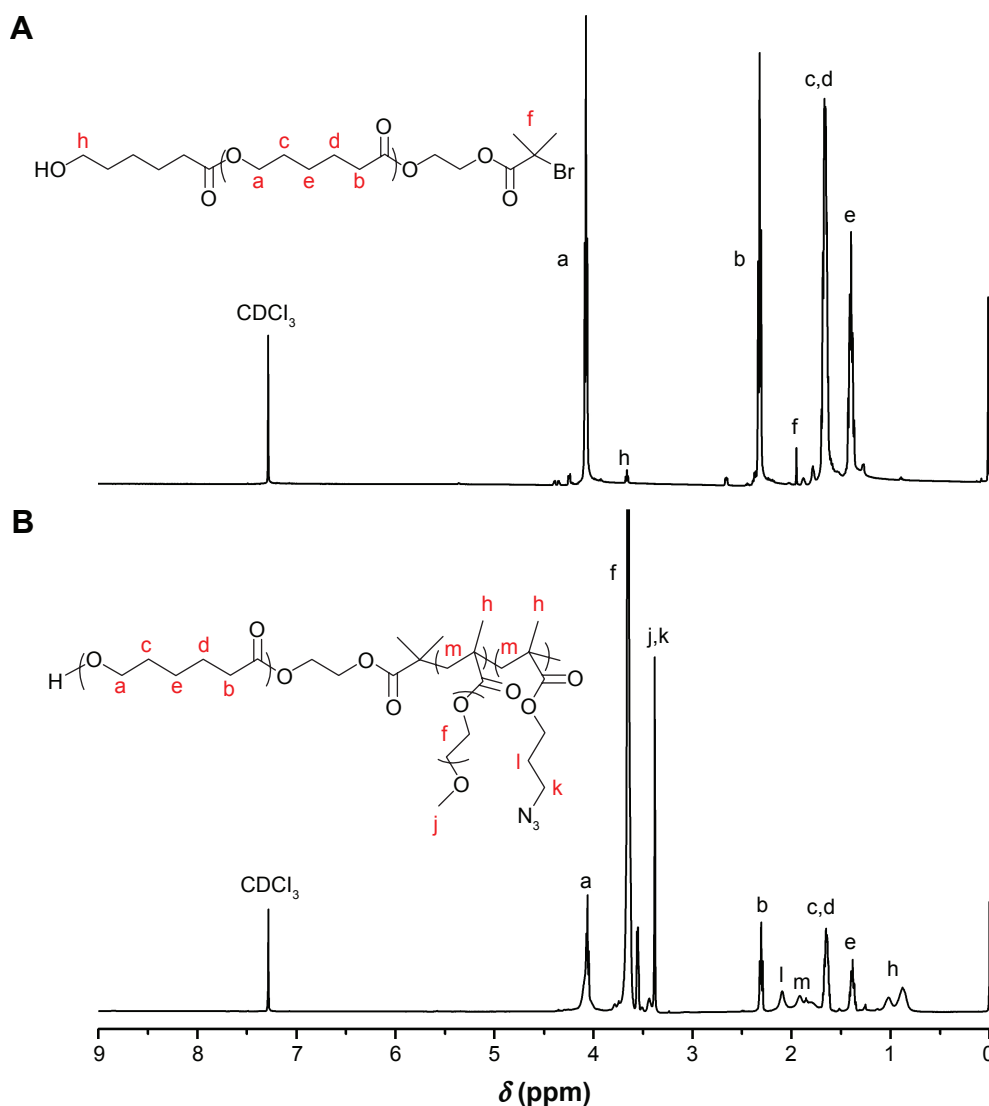


Figure 2 Proton nuclear magnetic resonance spectra of **(A)** PCL-Br and **(B)** PCL-b-P(OEGMA-co-AzPMA) in CDCl_3 .
Abbreviations: AzPMA, 3-azidopropyl methacrylate; OEGMA, oligo(ethylene glycol) ethyl methacrylate; PCL, polycaprolactone.

GPC, TEM and DLS. As revealed by the FT-IR spectra in Figure 3, it was clearly found that the peak at $2,100\text{ cm}^{-1}$ characteristic of the azide vibration almost disappeared, whereas three new peaks at $3,440$, $1,634$ and $1,560\text{ cm}^{-1}$ ascribed to Pt(IV) prodrug appeared after the shell cross-linking reaction, indicating the reaction of azide in the hydrophilic shell of copolymer with dialkyne cross-linker. Moreover, the SCL micelles were characterized by GPC with DMF as the elute. The GPC trace of SCL micelles is shown in Figure 1C. The molecular weight was shown to increase from $31,000\text{ g/mol}$ for PCL-b-P(OEGMA-co-AzPMA) to $491,000\text{ g/mol}$ for SCL micelles, providing another evidence for the successful cross-linking of PCL-b-P(OEGMA-co-AzPMA) shell.

To further confirm the success of shell cross-linking, TEM and DLS were employed to investigate the morphology and size of amphiphilic diblock copolymer micelles before

and after shell cross-linking. As seen from TEM images in Figure 4, under a drying state, both micelles revealed the formation of fairly monodisperse and spherical-shaped nanoparticles. The number-average diameters of SCL micelles and NCL micelles were determined to be 30 and 50 nm , respectively. The hydrophilic shell of SCL micelles was covalently cross-linked, and the molecular chains were packed. Thus, the diameter of SCL micelles was smaller than that of NCL micelles. As revealed by DLS results, it was also found that the average diameter of SCL micelles was smaller than that of NCL micelles after the shell cross-linking reaction, decreasing from 239.9 to 280.3 nm . The results revealed by DLS were in reasonable agreement with that obtained from TEM measurement. Both the results indicated that the diameter of SCL micelles was smaller than that of NCL micelles. It is worth noting that TEM technique

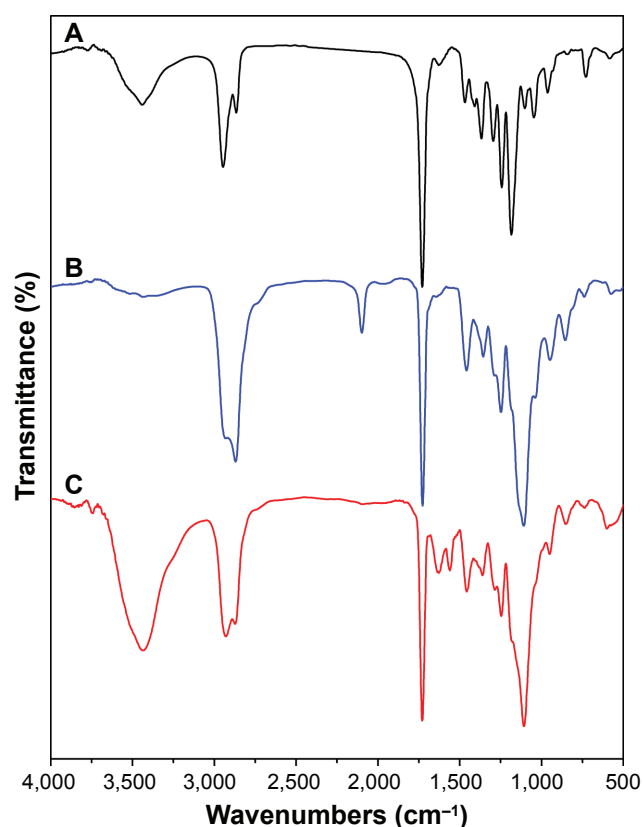


Figure 3 Fourier transform infrared spectra of (A) PCL-Br, (B) PCL-b-P(OEGMA-co-AzPMA) and (C) shell cross-linked micelles.

Abbreviations: AzPMA, 3-azidopropyl methacrylate; OEGMA, oligo(ethylene glycol) ethyl methacrylate; PCL, polycaprolactone.

determines nanoparticles dimension in the dry state, whereas DLS reports intensity-average dimension in solution, leading to results showing different sizes. Moreover, the hydrophilic shell of micelles was POEGMA, and was invisible under TEM measurement.⁴⁵ Meanwhile, to compare the structural stability of SCL micelles and NCL micelles, DMF, a good solvent for copolymer, was used in DLS measurements (Figure 4D). After both micelles were added in DMF, the NCL micelles dissociated into unimers and did not give any reading, whereas the SCL micelles still maintained the structural integrity, thus confirming the stabilization of micelles by shell cross-linking. The average diameter of SCL micelles was larger in DMF because the solvent DMF could swell SCL micelles by penetrating. Based on the above results, the obtained SCL micelles were successfully fabricated, and the structural stability was also confirmed.

In vitro drug release and cell uptake

In aqueous solution, the amphiphilic diblock copolymer could self-assemble into micelles with hydrophobic PCL as core and hydrophilic P(OEGMA-co-AzPMA) as shell. Thus, DOX was encapsulated in the hydrophobic core of micelles.

As described above, there were alkyne groups in Pt(IV) prodrug and azide groups in the shell of micelles. Then, shell cross-linking was carried out via the click reaction of azide groups in the shell of micelles with alkyne groups in Pt(IV) prodrug. Therefore, the SCL micelles could be utilized to achieve co-delivery of two different chemotherapeutic drugs; that is, DOX was loaded in the hydrophobic core of micelles via physical entrapment, while Pt(IV) prodrug was loaded in the hydrophilic shell of micelles via azide-alkyne click reaction. Thus, the obtained SCL micelles had two different drug-loading methods, physical entrapment and covalent loading of drug, exhibiting different drug release rates. To determine the LE and EE of DOX, a calibration curve was plotted for DOX/1 M HCl containing 10 mM VcNa solutions with different DOX concentrations, and then the content of DOX was determined according to the calibration curve. The amount of Pt(IV) prodrug was determined by TGA. As known, Pt is a thermally stable compound, while polymers typically decompose at temperatures $<400^{\circ}\text{C}$. As shown in Figure 5, it was found that cisplatin underwent a total weight loss of 34.7% at 500°C , indicating that only elemental platinum remained after 500°C . During the thermal analysis of SCL micelles, platinum of 5.5 wt % remained, which corresponds to about 8.5 wt % of cisplatin in the SCL micelles.

Due to the abundance of cellular reducing agents and low pH in endosomes/lysosomes, the cross-linker, Pt(IV) prodrug, can release cytotoxic Pt(II) species after the cellular uptake of SCL micelles loaded with DOX and Pt(IV),^{46,47} thus leading to micelles degradation and the release of DOX. Therefore, the drug release profile was investigated under mildly acidic and reducing environments in vitro (Figure 6). It was found that only 12.2% of Pt(IV) and 13.4% of DOX were released from SCL micelles within 72 h at pH 7.4. Then, in mildly acidic environments (pH 5.5), the release of Pt(IV) and DOX was relatively accelerated, and the amount of released Pt(IV) and DOX reached 24.3% and 40.0%, respectively. When sodium ascorbate was used as a reductant in solution, more significant acceleration of drug release was observed, and the most rapid release rate was observed at pH 5.5 with 5 mM sodium ascorbate. In the acidic and reducing condition, 60.4% of Pt(IV) and 92.7% of DOX were released within 72 h. It was worth noting that the amount of DOX released was higher than that of Pt(IV) prodrug; this was because DOX was loaded in the core of micelles via physical entrapment, while Pt(IV) prodrug was loaded in the shell of micelles via covalent cross-linking. The above results indicated that the Pt(IV) cross-linking shell could act as a diffusion barrier and block DOX burst release during blood circulation (pH 7.4 and low level of reducing

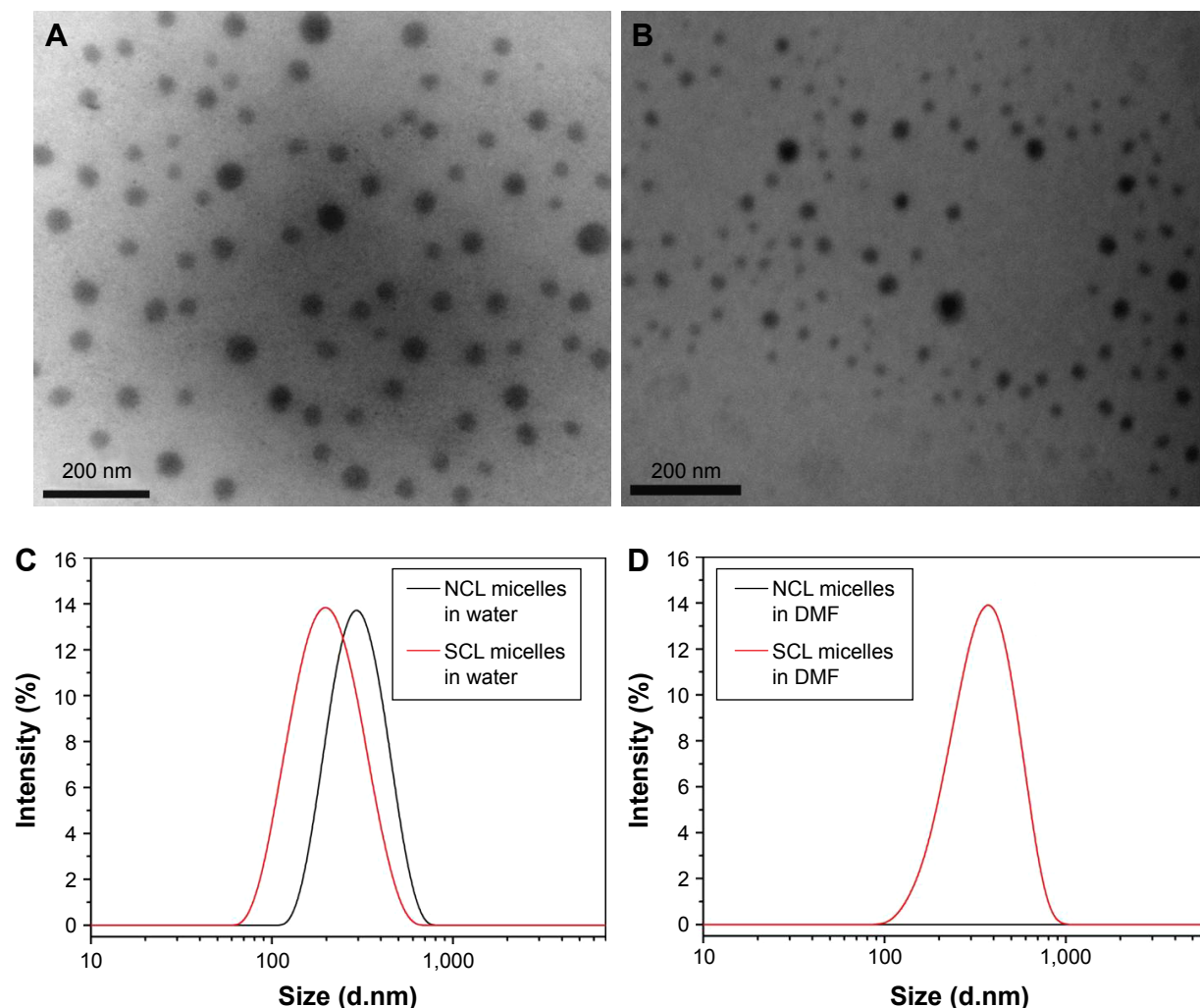


Figure 4 Transmission electron microscopy image of (A) NCL micelles and (B) SCL micelles. Dynamic light scattering curves of NCL and SCL micelles in water (C) and in DMF (D).

Abbreviations: DMF, dimethylformamide; NCL, non-cross-linked; SCL, shell cross-linked.

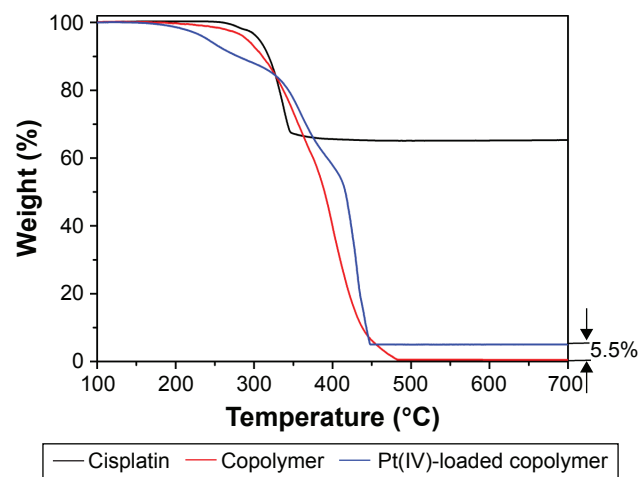


Figure 5 Thermogravimetric analysis curve of cisplatin, PCL-b-P(OEGMA-co-AzPMA) copolymer and Pt(IV) prodrug-loaded PCL-b-P(OEGMA-co-AzPMA) copolymer.

Abbreviations: AzPMA, 3-azidopropyl methacrylate; OEGMA, oligo(ethylene glycol) ethyl methacrylate; PCL, polycaprolactone; Pt, platinum.

agent), whereas in the presence of reducing agents and low pH in endosomes/lysosomes, Pt(IV) cross-linking shell would cleave, leading to enhanced cytotoxic accumulation of Pt(II) species and DOX release.

To examine the cellular internalization of SCL micelles, fluorescence microscopy study was conducted. As seen in Figure 7, the strong red fluorescence of DOX was observed within the cell nuclei, which contained blue DAPI. The cell nuclei turned red because DOX was bound to DNA. It was also found that there was little red fluorescence inside the cytoplasm. This is because the cross-linking shell of micelles was degraded under the mildly acidic pH inside endosomes and lysosomes and the highly reducing microenvironment in the cytosol.^{34,38,45} These results indicated that SCL micelles could effectively release DOX inside cells, and DOX was accumulated inside the cell nuclei.

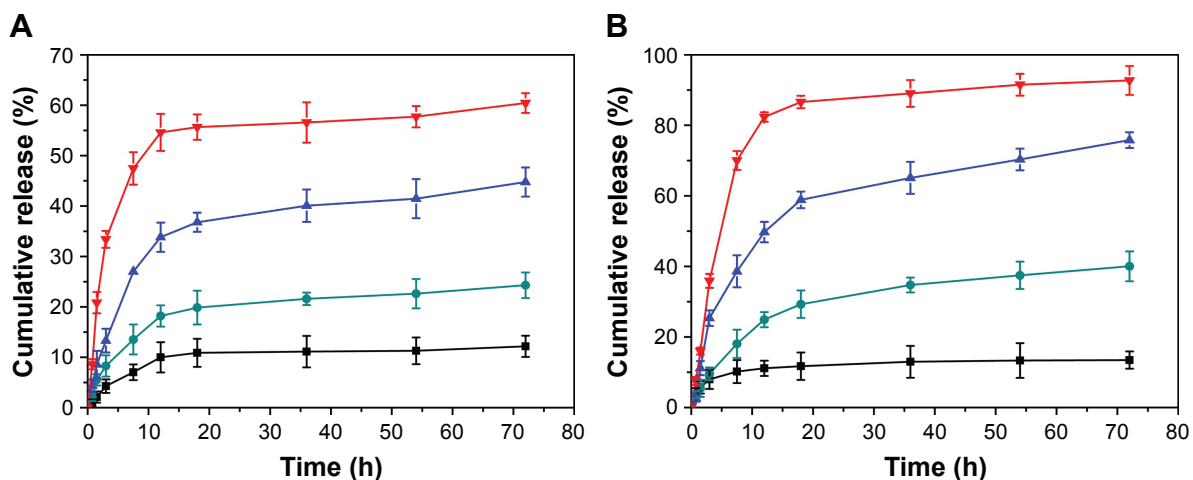


Figure 6 In vitro (A) Pt and (B) DOX release profiles of Pt(IV)- and DOX-loaded shell cross-linked micelles in aqueous solution at (■) pH 7.4, (●) pH 5.5, (▲) pH 7.4 with 5 mM sodium ascorbate and (▼) pH 5.5 with 5 mM sodium ascorbate.

Abbreviations: DOX, doxorubicin; Pt, platinum.

In vitro cell assay

The materials used as drug carriers in DDSs should be nontoxic, nonimmunogenic and preferably biodegradable. It is very important to evaluate the potential toxicity of

polymeric materials before they are applied as an effective drug carrier for the therapeutic treatment of tumors. When the drug carriers are applied to the body, they should be low or nontoxic to the normal tissue cells. In this study, the

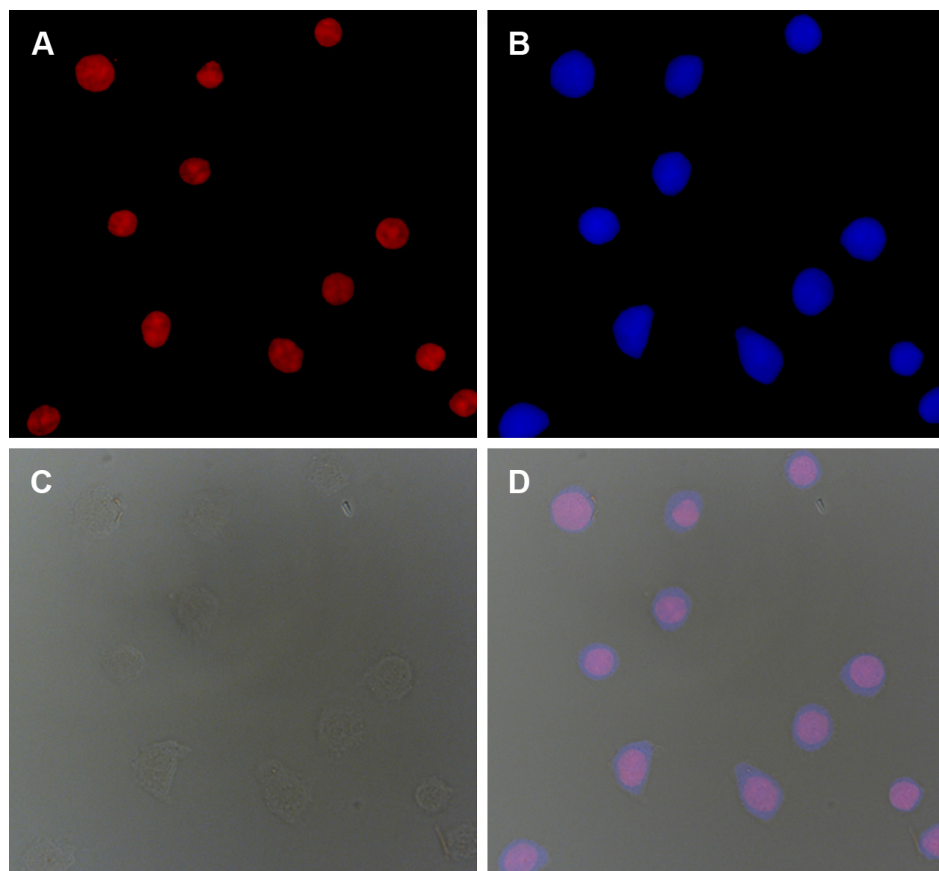


Figure 7 Fluorescence microscopy images of HeLa cells after incubation with DOX- and Pt(IV)-loaded shell cross-linked micelles for 6 h: (A) DOX (red), (B) cell nuclei stained by 4',6-diamidino-2-phenylindole (blue), (C) bright field and (D) overlay of (A–C).

Abbreviations: DOX, doxorubicin; Pt, platinum.

cytotoxicity of PCL-b-P(OEGMA-co-AzPMA) amphiphilic diblock copolymer against HeLa, A357 and HEK-293 cells was carefully investigated by the CCK-8 assays. As seen from Figure 8, PCL-b-P(OEGMA-co-AzPMA) showed no obvious cytotoxic effect on HeLa and A357 cells at a concentration range of 0.05–1.0 mg/mL. Even at the concentration of up to 5.0 mg/mL, the cell viability was above 80% after incubation for 72 h. In HEK-293 normal cells (Figure 8), although PCL-b-P(OEGMA-co-AzPMA) caused a slight decrease in the cell viability at the concentration of 1.0 mg/mL when the incubation time increased to 72 h, the cell viability was still nearly 70%. These results suggest that PCL-b-P(OEGMA-co-AzPMA) copolymers exhibit a good biocompatibility, and are suitable to be used as a platform for anticancer drugs.

The antitumor activity and synergistic effect of SCL micelles loaded with DOX and Pt(IV) at different drug concentrations and incubation times were studied in vitro using the CCK-8 assays. A357 and HeLa cells were first separately seeded in 96-well plates. After incubating for 24 h to allow cell attachment, the cells were treated with the free DOX, free PTX, DOX-loaded micelles, Pt(IV)-loaded micelles and SCL micelles loaded with both DOX and Pt(IV) containing different drug concentrations for 48 and 72 h. As shown in Figure 9, after 48 h incubation, all samples showed growth inhibition abilities against A357 and HeLa cells, and the cytotoxicity increased along with the increasing concentrations of drugs. Free single drug and single-drug-loaded micelles induced similar cytotoxicity,

demonstrating that the drug-loaded micelles could efficiently release drugs under acidic pH in endosomes/lysosomes and intracellular reduction. However, in contrast with free single drug and single-drug-loaded micelles, SCL micelles loaded with DOX and Pt(IV) showed higher cytotoxicity toward both A357 and HeLa cells, especially at low concentration. It was found that the cell viabilities of A357 and HeLa cells were 6.4% and 21.0%, respectively, after treatment with 1.0 μM of co-delivery drugs for 48 h, which were much lower than that of free single drug and single-drug-loaded micelles. It was worth noting that SCL micelles loaded with DOX and Pt(IV) containing 0.1 μM of drug concentration also showed an effective antitumor activity toward A357 and HeLa cells, exhibiting a robust enhancement of combination potency. Furthermore, with the increase in incubation time to 72 h, SCL micelles loaded with DOX and Pt(IV) showed more potent abilities of cellular growth inhibition against A357 and HeLa cells, which indicated that more Pt(IV) diesters released cytotoxic Pt(II) species under intracellular reduction and DOX could be further released from SCL micelles over time. Meanwhile, the distinguishing antitumor activity of single drugs and SCL micelles loaded with DOX and Pt(IV) could be seen from the IC_{50} values. As shown in Table 1, the IC_{50} values of SCL micelles loaded with DOX and Pt(IV) against A357 and HeLa cells at 48 h were 0.08 and 0.24 μM , respectively, which reduced to 0.02 and 0.09 μM at 72 h. Compared with free single drugs and single-drug-loaded micelles, SCL micelles loaded with DOX and Pt(IV) showed a much lower IC_{50} , indicating highest antitumor

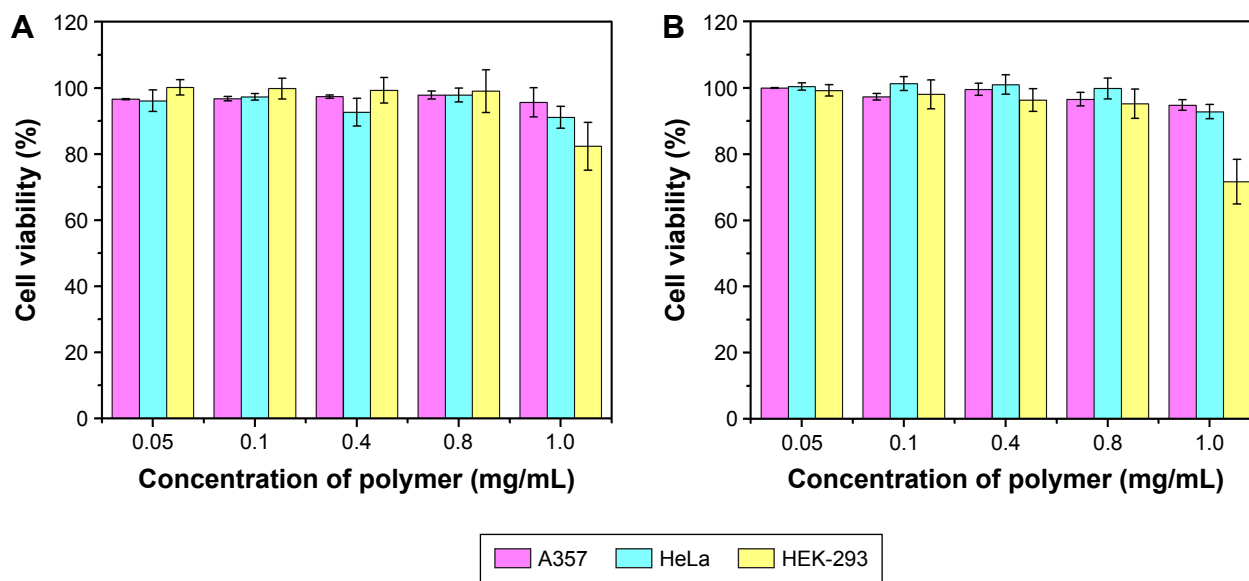


Figure 8 Cell cytotoxicity of PCL-b-P(OEGMA-co-AzPMA) against A357, HeLa and HEK-293 cells with different incubation times of (A) 48 and (B) 72 h. **Abbreviations:** AzPMA, 3-azidopropyl methacrylate; OEGMA, oligo(ethylene glycol) ethyl methacrylate; PCL, polycaprolactone.

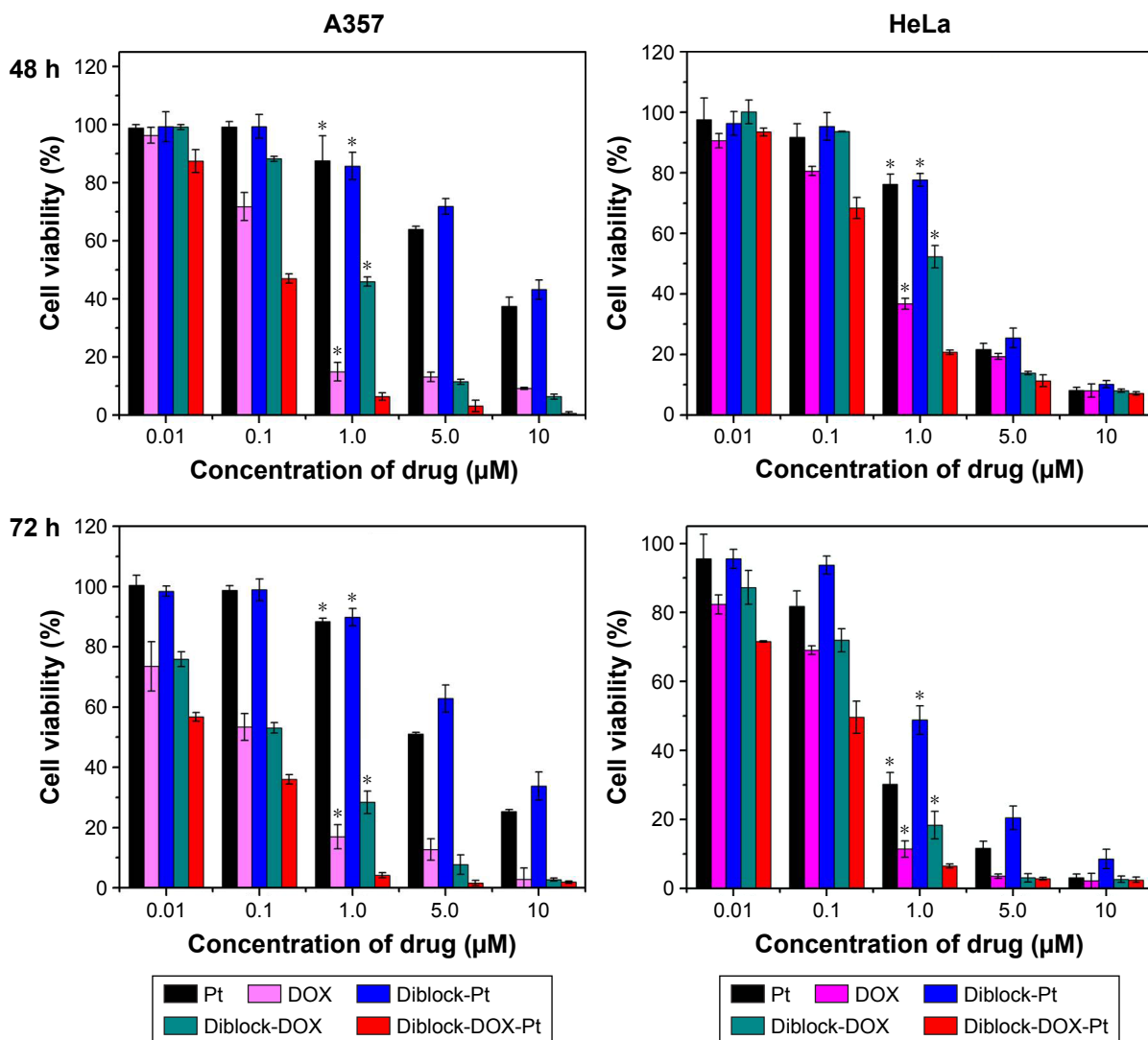


Figure 9 In vitro cell viability of A357 and HeLa cells against single drugs and shell cross-linked micelles loaded with DOX and Pt(IV) at different concentrations and incubation times. * $P < 0.05$ compared with diblock-DOX-Pt.

Abbreviations: DOX, doxorubicin; Pt, platinum.

activity. From the results discussed above, it is understood that SCL micelles loaded with DOX and Pt(IV) could significantly reduce cell viability even at very low concentrations, and outperform free single drugs and single-drug-loaded

micelles. These novel SCL micelles might provide a promising platform for co-delivery of multiple antitumor drugs and might have an important practical application in synergistic combination drug chemotherapy.

Table 1 IC_{50} values of single drugs and shell cross-linked micelles loaded with DOX and Pt(IV) corresponding to A357 and HeLa cells at different incubation times

Incubation time	Cells	IC_{50} (μM)				
		Free Pt	Free DOX	Pt(IV)-loaded micelles	DOX-loaded micelles	DOX- and Pt(IV)-loaded micelles
48 h	A357	7.19	0.24	8.46	0.81	0.08
72 h	A357	5.37	0.13	7.19	0.14	0.02
48 h	HeLa	2.16	0.50	2.33	1.09	0.24
72 h	HeLa	0.41	0.21	0.93	0.25	0.09

Abbreviations: DOX, doxorubicin; Pt, platinum.

Conclusion

In summary, SCL micelles prepared via the click reaction of azide group in the shell of micelles with alkyne groups in the Pt(IV) prodrug were employed as carriers to co-deliver DOX and Pt(IV) for combination cancer therapy. The results of FT-IR, GPC, TEM and DLS demonstrated that the structures of SCL micelles had hydrophilic PEG chains as shell and hydrophobic PCL as core encapsulating DOX. Studies on drug release showed that the drug release behavior of SCL micelles was pH- and reduction-sensitive, overcoming the drug burst release and achieving controlled drug release. The results of cellular uptake of the co-delivery SCL micelles further demonstrated that the micelles were effectively taken up by the cells and released drugs in the cells. The in vitro cell assay indicated that the diblock copolymer exerted no obvious cytotoxicity, and is suitable for use as drug carrier. The co-delivery SCL micelles caused much higher cell death in both HeLa and A357 tumor cells than free drug or single-drug-loaded micelles at the same dosage, exhibiting a synergistic combination of two drugs. The strategy of using anticancer drug as cross-linking linkage is a versatile approach to construct multidrug delivery systems, which might result in more efficient and patient-compliant cancer therapy.

Acknowledgments

The authors acknowledge the financial support from the National Natural Science Foundation of China (81372796) and the Shanghai Scientific and Technological Innovation Project (124119a2400).

Disclosure

The authors report no conflicts of interest in this work.

References

- Roussos ET, Condeelis JS, Patsialou A. Chemotaxis in cancer. *Nat Rev Cancer*. 2011;11:573–587.
- Lee MJ, Ye AS, Gardino AK, et al. Sequential application of anticancer drugs enhances cell death by rewiring apoptotic signaling networks. *Cell*. 2012;149:780–791.
- Thigpen JT, Brady MF, Homesley HD, et al. Phase III trial of doxorubicin with or without cisplatin in advanced endometrial carcinoma: a gynecologic oncology group study. *J Clin Oncol*. 2004;22:3902–3908.
- Wang AZ, Langer R, Farokhzad OC. Nanoparticle delivery of cancer drugs. *Annu Rev Med*. 2012;63:185–198.
- Prabhakar U, Maeda H, Jain RK, et al. Challenges and key considerations of the enhanced permeability and retention effect for nanomedicine drug delivery in oncology. *Cancer Res*. 2013;73:2412–2417.
- Dhal PK, Polomoscank SC, Avila LZ, et al. Functional polymers as therapeutic agents: concept to market place. *Adv Drug Deliv Rev*. 2009;61:1121–1130.
- Nicolas J, Mura S, Brambilla D, et al. Design, functionalization strategies and biomedical applications of targeted biodegradable/biocompatible polymer-based nanocarriers for drug delivery. *Chem Soc Rev*. 2013;42:1147–1235.
- Gottesman MM. Mechanisms of cancer drug resistance. *Annu Rev Med*. 2002;53:615–662.
- Woodcock J, Griffin JP, Behrman RE. Development of novel combination therapies. *N Engl J Med*. 2011;364:985–987.
- Ramasamy T, Haidar ZS, Tran TH, et al. Layer-by-layer assembly of liposomal nanoparticles with PEGylated polyelectrolytes enhances systemic delivery of multiple anticancer drugs. *Acta Biomater*. 2014;10:5116–5127.
- Ahmed F, Pakunlu RI, Brannan A, et al. Biodegradable polymersomes loaded with both paclitaxel and doxorubicin permeate and shrink tumors, inducing apoptosis in proportion to accumulated drug. *J Control Release*. 2006;116:150–158.
- Larson N, Roberts S, Ray A, et al. In vitro synergistic action of geldanamycin and docetaxel-containing HPMA copolymer-RGDfK conjugates against ovarian cancer. *Macromol Biosci*. 2014;14:1735–1747.
- Al-Lazikani B, Banerji U, Workman P. Combinatorial drug therapy for cancer in the post-genomic era. *Nat Biotechnol*. 2012;30:1–13.
- Katragadda U, Fan W, Wang YZ, Teng Q, Tan C. Combined delivery of paclitaxel and tanespimycin via micellar nanocarriers: pharmacokinetics, efficacy and metabolomic analysis. *PLoS One*. 2013;8:5861–5869.
- Morton SW, Lee MJ. A nanoparticle-based combination chemotherapy delivery system for enhanced tumor killing by dynamic rewiring of signaling pathways. *Sci Signal*. 2014;7:ra44.
- Goldberg M, Mahon K, Anderson D. Combinatorial and rational approaches to polymer synthesis for medicine. *Adv Drug Deliv Rev*. 2008;60:971–978.
- Zhao Y, Sakai F, Su L, et al. Progressive macromolecular self-assembly: from biomimetic chemistry to bio-inspired materials. *Adv Mater*. 2013;25:5215–5256.
- Yu J, Deng H, Xie F, et al. The potential of pH-responsive PEG-hyperbranched polyacylhydrazone micelles for cancer therapy. *Biomaterials*. 2014;35:3132–3144.
- Tomcin S, Kelsch A, Staff H, et al. HPMA-based block copolymers promote differential drug delivery kinetics for hydrophobic and amphiphilic molecules. *Acta Biomater*. 2016;35:12–22.
- Kataoka K, Harada A, Nagasaki Y. Block copolymer micelles for drug delivery: design, characterization and biological significance. *Adv Drug Deliv Rev*. 2001;47:113–131.
- Wang H, Zhao Y, Wu Y, et al. Enhanced anti-tumor efficacy by co-delivery of doxorubicin and paclitaxel with amphiphilic methoxy PEG-PLGA copolymer nanoparticles. *Biomaterials*. 2011;32:8281–8290.
- Conte C, Ungaro F, Maglio G, et al. Biodegradable core-shell nano-assemblies for the delivery of docetaxel and Zn(II)-phthalocyanine inspired by combination therapy for cancer. *J Control Release*. 2013;167:40–52.
- Zhou L, Cheng R, Tao H, et al. Endosomal pH-activatable poly(ethylene oxide)-graft-doxorubicin prodrugs: synthesis, drug release, and biodistribution in tumor-bearing mice. *Biomacromolecules*. 2011;12:1460–1467.
- Liu T, Li XJ, Qian Y, Hu X, Liu S. Multifunctional pH-disintegrable micellar nanoparticles of asymmetrically functionalized β -cyclodextrin-based star copolymer covalently conjugated with doxorubicin and DOTA-Gd moieties. *Biomaterials*. 2012;33:2521–2531.
- Hu W, Qiu LP, Cheng L, et al. Redox and pH dual responsive poly(amidoamine) dendrimer-poly(ethylene glycol) conjugates for intracellular delivery of doxorubicin. *Acta Biomater*. 2016;36:241–253.
- Wei H, Quan CY, Chang C, et al. Preparation of novel ferrocene-based shell cross-linked thermoresponsive hybrid micelles with antitumor efficacy. *J Phys Chem B*. 2010;114:5309–5314.
- O'Reilly RK, Hawker CJ, Wooley KL. Cross-linked block copolymer micelles: functional nanostructures of great potential and versatility. *Chem Soc Rev*. 2006;35:1068–1083.
- Duong HTT, Marquis CP, Whittaker MR, Davis TP, Boyer C. Acid degradable and biocompatible polymeric nanoparticles for the potential codelivery of therapeutic agents. *Macromolecules*. 2011;44:8008–8819.

29. Owen SC, Chan DPY, Shoichet MS. Polymeric micelle stability. *Nano Today*. 2012;7:53–65.
30. Wu Y, Chen W, Meng F, et al. Core-crosslinked pH-sensitive degradable micelles: a promising approach to resolve the extracellular stability versus intracellular drug release dilemma. *J Control Release*. 2012;164:338–345.
31. Li WM, Chen SY, Liu DM. In situ doxorubicin–CaP shell formation on amphiphilic gelatin–iron oxide core as a multifunctional drug delivery system with improved cytocompatibility, pH-responsive drug release and MR imaging. *Acta Biomater*. 2013;9:5360–5368.
32. Sun CX, Shu K, Wang W, et al. Encapsulation and controlled release of hydrophilic pesticide in shell cross-linked nanocapsules containing aqueous core. *Int J Pharm*. 2014;463:108–114.
33. Sakai S, Taya M. On-cell surface cross-linking of polymer molecules by horseradish peroxidase anchored to cell membrane for individual cell encapsulation in hydrogel sheath. *ACS Macro Lett*. 2014;3:972–975.
34. Liao LY, Liu J, Dreaden EC, et al. A convergent synthetic platform for single-nanoparticle combination cancer therapy: ratiometric loading and controlled release of cisplatin, doxorubicin, and camptothecin. *J Am Chem Soc*. 2014;136:5896–5899.
35. Nystrom AM, Wooley KL. Thiol-functionalized shell crosslinked knedel-like (SCK) nanoparticles: a versatile entry for their conjugation with biomacromolecules. *Tetrahedron*. 2008;64:8543–8552.
36. Abdullah NA, Nam J, Mok H, Lee YK, Park SY. Dual-responsive crosslinked pluronic micelles as a carrier to deliver anticancer drug taxol. *Macromol Res*. 2013;21:92–99.
37. Kozielski KL, Tzeng SY, De Mendoza BA, Green JJ. Bioreducible cationic polymer-based nanoparticles for efficient and environmentally triggered cytoplasmic siRNA delivery to primary human brain cancer cells. *ACS Nano*. 2014;8:3232–3241.
38. Segal E, Pan HZ, Benayoun L, et al. Enhanced anti-tumor activity and safety profile of targeted nano-scaled HPMA copolymer-alendronate-TNP-470 conjugate in the treatment of bone malignancies. *Biomaterials*. 2011;32:4450–4463.
39. Eldar-Boock A, Polyak D, Scomparin A, Satchi-Fainaro R. Nano-sized polymers and liposomes designed to deliver combination therapy for cancer. *Curr Opin Biotechnol*. 2013;24:682–689.
40. Lehar J, Krueger AS, Avery W, et al. Synergistic drug combinations tend to improve therapeutically relevant selectivity. *Nat Biotechnol*. 2009;27:659–666.
41. Sahoo SK, Acharya S. Sustained targeting of Bcr-Abl+ leukemia cells by synergistic action of dual drug loaded nanoparticles and its implication for leukemia therapy. *Biomaterials*. 2011;32:5643–5662.
42. Lee SM, O'Halloran TV, Nguyen ST. Polymer-caged nanobins for synergistic cisplatin-doxorubicin combination chemotherapy. *J Am Chem Soc*. 2010;132:17130–17138.
43. Xiao H, Li W, Qi R, et al. Co-delivery of daunomycin and oxaliplatin by biodegradable polymers for safer and more efficacious combination therapy. *J Control Release*. 2012;163:304–314.
44. Chen WL, Zhang JZ, Hu JH, Guo QS, Yang D. Preparation of amphiphilic copolymers for covalent loading of paclitaxel for drug delivery system. *J Polym Sci Polym Chem*. 2014;52:366–374.
45. Hu XL, Li H, Luo SZ, Liu T, Jiang YY, Liu SY. Thiol and pH dual-responsive dynamic covalent shell cross-linked micelles for triggered release of chemotherapeutic drugs. *Polym Chem*. 2013;4:695–706.
46. Hall MD, Hambley TW. Platinum(IV) antitumour compounds: their bioinorganic chemistry. *Coord Chem Rev*. 2002;232:49–67.
47. Hall MD, Alderden RA, Callaghan R, et al. The fate of platinum(II) and platinum(IV) anti-cancer agents in cancer cells and tumours. *J Struct Biol*. 2006;155:38–44.

Supplementary materials

Preparation of platinum(IV) (Pt[IV]) prodrug containing difunctional alkyne

Pt(IV) prodrug containing difunctional alkyne was prepared according to the referenced methods.¹⁻⁴ In the first procedure, cisplatin (1.0 g, 3.05 mmol) was added to 3.5 mL of H₂O₂ 30 w/v. The mixture was stirred at 70°C for 5 h and then at room temperature overnight. After filtration and washing with ice cold water, ethanol, and diethyl ether, the bright yellow powder oxoplatin (Pt(NH₃)₂Cl₂(OH)₂) was obtained (yield 0.85 g, 83.4%).

In a second procedure, succinic anhydride (684 mg, 6.834 mmol) was added to a suspension of oxoplatin (600 mg, 1.8 mmol) in dimethylformamide (15 mL). The mixture was stirred at 70°C for 24 h. The solution was concentrated under vacuum and precipitated into cold diethyl ether. After filtration, the product (Pt(NH₃)₂Cl₂(OOCCH₂CH₂COOH)₂) was dried in vacuo overnight, yielding a pale-yellow solid (431.6 mg, yield of 93.0%).

In a third procedure, (Pt(NH₃)₂Cl₂(OOCCH₂CH₂COOH)₂) (217 mg, 0.5 mmol) in dimethylformamide, DIC (247 mg,

1.2 mmol) and N-hydroxysuccinimide (NHS) (138 mg, 1.2 mmol) was added to a solution of Pt(IV) compound. The reaction mixture was stirred at room temperature overnight, and then propargylamine (110 mg, 2 mmol) was added. After another 24 h, the solution was concentrated under vacuum and precipitated into cold diethyl ether. After filtration, a Pt(IV) prodrug soluble in water (yield 180 mg, 75.0%) containing difunctional alkyne was obtained. Proton nuclear magnetic resonance (δ , ppm, 400 MHz, dimethylsulfoxide-*d*₆): 6.12-5.80 (6H, NH₃), 3.23 (2H, CH₂CCH), 2.60 (2H, OOCCH₂), 2.39 (2H, NHCOCH₂), 2.13 (1H, CCH).

References

1. Shi Y, Liu SA, Kerwood DJ, Goodisman J, Dabrowiak JC. Pt(IV) complexes as prodrugs for cisplatin. *J Inorg Biochem.* 2012;107(1):6–14.
2. Rieter WJ, Pott KM, Taylo KM, Lin W. Nanoscale coordination polymers for platinum-based anticancer drug delivery. *J Am Chem Soc.* 2008;130(35):11584–11585.
3. Dhar S, Daniel WL, Giljohann DA, Mirkin CA, Lippard SJ. Polyvalent oligonucleotide gold nanoparticle conjugates as delivery vehicles for platinum(IV) warheads. *J Am Chem Soc.* 2009;131(41):14652–14653.
4. Duong HT, Huynh VT, de Souza P, Stenzel MH. Core-cross-linked micelles synthesized by clicking bifunctional Pt(IV) anticancer drugs to isocyanates. *Biomacromolecules.* 2010;11(9):2290–2299.

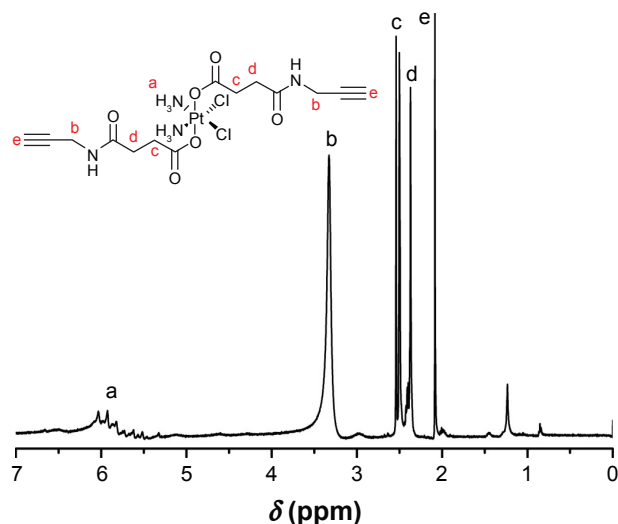


Figure S1 ¹H NMR spectra of Pt(IV) containing difunctional alkyne.
Abbreviation: ¹H NMR, proton nuclear magnetic resonance.

International Journal of Nanomedicine

Publish your work in this journal

The International Journal of Nanomedicine is an international, peer-reviewed journal focusing on the application of nanotechnology in diagnostics, therapeutics, and drug delivery systems throughout the biomedical field. This journal is indexed on PubMed Central, MedLine, CAS, SciSearch®, Current Contents®/Clinical Medicine,

Submit your manuscript here: <http://www.dovepress.com/international-journal-of-nanomedicine-journal>

Dovepress

Journal Citation Reports/Science Edition, EMBase, Scopus and the Elsevier Bibliographic databases. The manuscript management system is completely online and includes a very quick and fair peer-review system, which is all easy to use. Visit <http://www.dovepress.com/testimonials.php> to read real quotes from published authors.